

**REPUBLIC OF AZERBAIJAN**

*On the rights of the manuscript*

**ABSTRACT**

of the dissertation for the degree of Doctor of Philosophy in Physics

**CHARACTERISTICS OF ELECTRICAL, PHOTOELECTRIC  
AND OPTICAL PROPERTIES OF  $CuIn_5S_8$  AND  $Cu_3In_5S_9$   
CRYSTALS**

Speciality: 2211.01 – Solid-state physics

Field of science: Physics

Applicant: **Aynura Isa Bayramova**

**Baku – 2024**

The work was performed at Azerbaijan University of Architecture and Construction and Baku State University.

Scientific supervisor:

Doctor of Physical and Mathematical Sciences, Professor

**Panahov Tahir Musa**

Doctor of Physics Sciences (Professor)

**Huseynov Ali Hasan**

**Official opponents:**



Doctor of Physics Sciences (Professor),

**Huseynov Jahangir Islam**

Doctor of Physical Sciences (Professor),

**Babayeva Rena Fikrat**

Doctor of Philosophy in Physics

**Mammadov Vusal Usub**

Dissertation council ED 2.19 of Supreme Attestation Commission under the President of the Republic of Azerbaijan operating at Baku State University

Chairman of the Dissertation council:

Doctor of physical sciences,  
associate professor

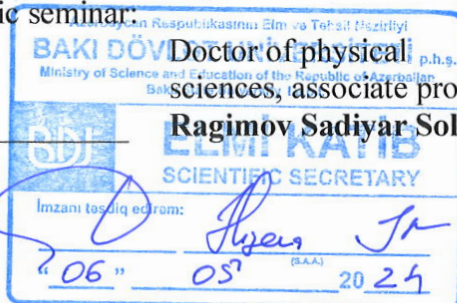
**Mammadov Huseyn Mikayil**

Scientific secretary of the Dissertation council:

Doctor of philosophy in  
physics

**Hajiyeva Shahla Nabi**

Chairman of the scientific seminar:



Doctor of physical  
sciences, associate professor

**Ragimov Sadiyar Soltan**

## GENERAL DESCRIPTION OF WORK

**The actuality of the subject and degree of elaboration.** The study of the Cu-In-S ternary system is mainly related to the studies of the  $\text{CuInS}_2$  ternary compound, which has semiconducting properties and great practical importance. The fundamental absorption region of the  $\text{CuInS}_2$  compound crystal is located in the near-infrared region of electromagnetic radiation, and has a record high value of the absorption coefficient among semiconductor compounds. Therefore, crystal is the most suitable material for making high-efficiency photoelectric converter and has great practical importance. The  $\text{CuInS}_2$  compound is slightly non-stoichiometric and crystallizes in the chalcopyrite structure. In the  $\text{A}^{\text{I}}\text{-B}^{\text{III}}\text{-C}^{\text{VI}}$  system, it was shown that the simple chalcopyrite structure for the formula  $\text{A}^{\text{I}}\text{B}^{\text{III}}\text{C}^{\text{VI}}_2$  does not exist only in the  $\text{CuInS}_2$  composition.  $\text{CuInS}_2$  is found in nature as the mineral roxite. This compound forms a sphalerite-type structure at high pressure and high temperature, and this structure is characterized by a high degree of defects. In the Cu-In-S ternary system, it has been shown by various researchers that there are stable phases such as  $\text{CuIn}_3\text{S}_5$ ,  $\text{CuIn}_5\text{S}_8$ ,  $\text{Cu}_3\text{In}_5\text{S}_9$ , and  $\text{Cu}_2\text{In}_4\text{S}_7$ . In the state diagram of the  $\text{Cu}_2\text{S}$ - $\text{In}_2\text{S}_3$  quasi-binary system, there is a distectic point on the liquidus line in the state diagram containing 29.1 at.% In. The stoichiometric chemical formula of the  $\tau_4$ -phase, which has a certain region of homogeneity around this point, corresponds to  $\text{Cu}_3\text{In}_5\text{S}_9$ . This phase crystallizes in the space group ( $m\bar{3}17$ ) and belongs to the group of layered crystals.<sup>1</sup>

Another phase observed in the  $\text{Cu}_2\text{S}$ - $\text{In}_2\text{S}_3$  quasibinary system is the  $\text{CuIn}_5\text{S}_8$  compound. It has a structure similar to the crystal structure of the spinel mineral, which has 56 atoms in the elementary core of the crystal. The close-packing of atoms causes 25% vacancies in the anion sublattice. Therefore,  $\text{CuIn}_5\text{S}_8$  crystal belongs to the

---

<sup>1</sup> Fiechter S., Diesner K., Tomm Y., Inst. Phys. Conf. Ser., Ternary and Multinary Compounds. Section A. Cryst. Growth and Characterization, -1998, -152, p.-27-30

category of defective crystals. Due to their photosensitivity and resistance to radiation, these crystals are used as a photocatalyst material in the production of hydrogen through the electrolysis of water. 11.6% vacancies were determined in the anion sublattice in the crystal structure of the  $\text{Cu}_3\text{In}_5\text{S}_9$  compound, which is an intermediate state of the  $\text{CuIn}_5\text{S}_8$  compound and the  $\text{CuInS}_2$  compound with a normal chalcopyrite structure, which meets the normal valency condition. From this, it can be concluded that the  $\text{Cu}_3\text{In}_5\text{S}_9$  compound can include the properties of other compounds.

Due to their photoelectric properties,  $\text{CuIn}_5\text{S}_8$  and  $\text{Cu}_3\text{In}_5\text{S}_9$  compounds have a number of important aspects. The  $\text{CuIn}_5\text{S}_8$  crystal has a spinel type structure. Due to close packing of atoms in the crystal structure, 25% vacancies are created in the anion sublattice.  $\text{Cu}_3\text{In}_5\text{S}_9$  crystals have a layered structure and a hexagonal syngonium structure. There are 11.6% anion vacancies in the anion sublattice of this crystal. The high concentration of anion vacancies in the crystal structure creates certain characteristics in the optical and photoelectric properties of the crystal and almost eliminates the role of foreign impurity atoms. The study of the fundamental parameters of  $\text{CuIn}_5\text{S}_8$  and  $\text{Cu}_3\text{In}_5\text{S}_9$  crystals shows that the crystals are practically promising materials from the point of view of making high-efficiency and high-frequency photoelectric converters and Solar cells. From another aspect, the complex study of  $\text{CuIn}_5\text{S}_8$  and  $\text{Cu}_3\text{In}_5\text{S}_9$  thin films and crystals is included in the framework of current problems. It was possible to increase the efficiency of the reaction in photocatalysts made on the basis of metal nanoparticles with these materials in hydrogen production by electrocatalytic water splitting to 3.6%, and scientific researches are being continued to raise this value to higher levels.

In accordance with the intended purpose in the dissertation work, the technologies of synthesis of  $\text{CuIn}_5\text{S}_8$  and  $\text{Cu}_3\text{In}_5\text{S}_9$  complex chalcogenide compounds, growing of monocrystals and obtaining of thin films and the Ag nanoparticles production technology were developed. Microstructure and X-ray structural analyzes were performed on the obtained samples. Electrical, photoelectric and optical properties of  $\text{CuIn}_5\text{S}_8$  and  $\text{Cu}_3\text{In}_5\text{S}_9$  crystals and thin layers

have been comprehensively studied, promising practical application areas have been shown by revealing the features in their properties. The technology of obtaining Ag nanoparticles by modified chemical deposition method has been developed. The photocatalysts prepared on the basis of  $\text{CuIn}_5\text{S}_8 - \text{Ag}(\text{Np})$  and  $\text{Cu}_3\text{In}_5\text{S}_9 - \text{Ag}(\text{Np})$  multilayer structures were used in the electrophotocatalytic decomposition of water and the efficiency of the reactions was determined. The issues raised in the dissertation work have been fully fulfilled.

**The object and subject of the research:** Tri-component compounds based on group I, III and VI elements attract the attention of more researchers in search of semiconductor materials for the preparation of high-efficiency solar energy converters. The fundamental parameters of some of the compounds of type  $\text{A}^{\text{I}}\text{B}^{\text{III}}\text{C}^{\text{VI}}_2$ ,  $\text{A}^{\text{I}}\text{B}^{\text{III}}_5\text{C}^{\text{VI}}_8$  and  $\text{A}^{\text{I}}_3\text{B}^{\text{III}}_5\text{C}^{\text{VI}}_9$  are very close to those required for ideal conversion of solar radiation. Considering this point, compounds  $\text{CuIn}_5\text{S}_8$  and  $\text{Cu}_3\text{In}_5\text{S}_9$  were chosen as research objects. The chemically stable  $\text{CuIn}_5\text{S}_8$  phase formed in the Cu – In – S system crystallizes in chain structures, while  $\text{Cu}_3\text{In}_5\text{S}_9$  crystallizes in layered structures. Their comparative study also represents theoretical interest.

**Purposes and tasks of research:** The main purposes of the dissertation was to study the electrical, photoelectric and optical properties of crystal ingots and thin films of  $\text{CuIn}_5\text{S}_8$  and  $\text{Cu}_3\text{In}_5\text{S}_9$  chemically stable compounds with a defective crystal structure in the  $\text{Cu}_2\text{S} - \text{In}_2\text{S}_3$  quasibinary system in wide temperature and optical excitation ranges and to identify their properties and determine their practical applications. To achieve this goal, the following problems were solved:

1. Processing the optimal technology for the synthesis and growth of monocrystals of the compounds  $\text{CuIn}_5\text{S}_8$  and  $\text{Cu}_3\text{In}_5\text{S}_9$ . Growing thin films of compounds with the condition of maintaining the stoichiometric composition by the method of rapid thermal evaporation in vacuum. Obtaining information about the composition and structure of the grown crystals and thin films by performing XRD, EDAX, microstructure and optical spectroscopy analyses;

2. Determination of resistance and Hall conductivity in a wide temperature range of electrical properties to identify the mechanism of electrical conductivity in  $\text{CuIn}_5\text{S}_8$  and  $\text{Cu}_3\text{In}_5\text{S}_9$  crystals;

3. Determining the parameters of non-equilibrium charge carriers in  $\text{CuIn}_5\text{S}_8$  and  $\text{Cu}_3\text{In}_5\text{S}_9$  crystals and thin films in a wide range of optical excitation, including under the influence of laser radiation and by studying the spectrum and kinetics of the photocurrent in stationary and non-stationary modes;

4. Identification of radiative recombination channels as a result of the study of photoluminescence spectra in  $\text{CuIn}_5\text{S}_8$  and  $\text{Cu}_3\text{In}_5\text{S}_9$  crystals and thin films;

5. Preparation of nanoparticle photocatalysts based on  $\text{CuIn}_5\text{S}_8$  and  $\text{Cu}_3\text{In}_5\text{S}_9$  thin films and determination of their efficiency in the reaction of hydrogen production by water splitting.

**Research methods :** To perform of the dissertation work were used the methods such as XRD, EDAX, microstructure and optical spectroscopy analyses, four-contact resistance measurement, determination of the type and mobility of charge carriers by the Hall current method and measurement of stationary and non-stationary photocurrent and luminescence spectra using by modern pulse Nd:YAG SOLARIS laser, semiconductor permanent lasers, double dispersion M833 type diffraction monochromator, Le Croy and TECTRONIK types memory digital oscillographs with type memory, S7031-1006S -type HAMAMATSU photodetector made in Japan and computer equipment with special programs.

Monocrystals and thin films of  $\text{CuIn}_5\text{S}_8$  and  $\text{Cu}_3\text{In}_5\text{S}_9$  were used as research objects. The elements of both compounds in stoichiometric proportions were synthesized by us using a special technological method by melting the elements in a quartz ampoule with air suction and a closed mouth. Monocrystals of the synthesized compounds were obtained by slow cooling methods in a Bridgman and constant temperature gradient furnace. Since there is 25% vacancy in the anion sublattice of  $\text{CuIn}_5\text{S}_8$  crystal and 11.6% vacancy in  $\text{Cu}_3\text{In}_5\text{S}_9$  crystals, the crystals show neutrality towards foreign impurities. Compounds have a congruent melting point and a distectic point on the liquidus curve. Therefore, monocrystal growth

and thin film acquisition technology do not require complex equipment. Thin films of the compounds were obtained by us on various substrates by the method of rapid thermal evaporation in vacuum. In the scientific literature, there are numerous materials on the fact that crystals and thin films are promising research objects as high-efficiency photoelectric converters, photocatalysts, and intense luminescent materials.

### **The main provisions submitted to the defense:**

1.  $\text{CuIn}_5\text{S}_8$  crystal and thin film is a promising material for the development of wide-band and high-efficiency photoconverters that can operate in the energy range of photons of natural radiation  $h\nu = 0.8...2.7$  eV.

2. The absorption band observed at 0.99 eV energy in the absorption spectrum of the  $\text{CuIn}_5\text{S}_8$  thin film formed by rapid thermal evaporation in vacuum and deposition on the liquid phase is stimulated by the transition of electrons from the valence band to the donor level.

3. It is of great practical interest to develop a high-efficiency converter for the conversion of p-Si/n- $\text{CuIn}_5\text{S}_8$  tandem photovoltaic solar radiation into electrical energy.

4. Since the lifetime of the fast recombination centers at a high level of optical excitation is 20 ns in the  $\text{Cu}_3\text{In}_5\text{S}_9$  crystal, this crystal can be used as a high-frequency photoelectric converter.

5. In the reaction with the  $\text{Zn}/\text{CuIn}_5\text{S}_8/\text{TiO}_2$  structured photocatalyst electrode, the efficiency of the reaction in the production of  $\text{H}_2$  by water splitting was 3.6%, in the reaction with the  $\text{Zn}/\text{Cu}_3\text{In}_5\text{S}_9/\text{Ag}(\text{Np})$  structured photocatalyst electrode and in the p-Ge/ $\text{CuIn}_5\text{S}_8/\text{Ag}(\text{Np})$  -structured photocatalyst electrodes was 2.8 and 3.2 %, respectively .

6. In the reaction with the  $\text{Zn}/\text{Cu}_3\text{In}_5\text{S}_9/\text{Ag}(\text{Np})$  structured positive potential photocatalyst electrode, the efficiency of the reaction in the production of  $\text{H}_2$  by water splitting was determined to be 2.9%. The low surface roughness of  $\text{Cu}_3\text{In}_5\text{S}_9$  thin films leads to low efficiency of electrolysis.

## Scientific novelty of the study:

The technology of obtaining  $\text{CuIn}_5\text{S}_8$  and  $\text{Cu}_3\text{In}_5\text{S}_9$  crystals and thin films was developed and for the first time a thin film of  $\text{CuIn}_5\text{S}_8$  was obtained on the surface of the liquid phase substrate;

- Mechanisms of current conduction in a wide temperature range have been determined in  $\text{CuIn}_5\text{S}_8$  and  $\text{Cu}_3\text{In}_5\text{S}_9$  crystals. In the center of Brillouin zone of  $\text{CuIn}_5\text{S}_8$  crystals, the energetic band diagram is constructed;

- In  $\text{CuIn}_5\text{S}_8$  and  $\text{Cu}_3\text{In}_5\text{S}_9$  crystals, nanosecond relaxations of photocurrents in high-level optical excitation were detected and the mechanism of the phenomenon was determined;

- In  $\text{Cu}_3\text{In}_5\text{S}_9$  crystals, high-intensity photoluminescence and a band belonging to triplet-type excitons were observed in the high-energy region of the luminescence spectrum;

- Ag nanoparticles were obtained by reaction with polyol and they were used in the preparation of photocatalysts with metal/semiconductor/Ag(Np) structure and applied in  $\text{H}_2$  production.

**The theoretical and practical significance of the study** consists in revealing the regularities of the role of cation and anion vacancies in solid bodies with a complex composition with defect structure, which shape the physical properties of the crystal, and showing ways to determine the effect of the donor and acceptor-type levels created by such vacancies on the radiative recombination of non-equilibrium charge carriers in the conditions of high optical excitation. In the dissertation work, the possibility of preparing  $p\text{-Si}/n\text{-CuIn}_5\text{S}_8$  tandem photocell, ultra-high frequency photoresistors based on  $\text{CuIn}_5\text{S}_8$  and  $\text{Cu}_3\text{In}_5\text{S}_9$  crystals and  $\text{Zn}/\text{CuIn}_5\text{S}_8/\text{TiO}_2$ ,  $\text{Zn}/\text{Cu}_3\text{In}_5\text{S}_9/\text{Ag}(\text{Np})$ ,  $p\text{-Ge}/\text{CuIn}_5\text{S}_8/\text{Ag}(\text{Np})$  structured photocatalysts was shown.

**Approbation and application:** 14 scientific works of the author have been published on the subject of the dissertation, including 2 articles in journals indexed in the international "Web of Science" database, 5 articles in republican journals, 7 in international

and republican level conference materials (see the list of scientific works published on the subject of the dissertation).

**The structure and volume of the dissertation :** Dissertation work consist of 150 pages in computer text volume, 206823 marks excluding tables, pictures, bibliography list, conditional marks, Introduction - 14774 marks, Chapter I - 43368 marks, Chapter II - 34849 marks, Chapter III - 50145 marks, Chapter IV - 33818 marks , and a list of literature used in 138 titles.

## THE MAIN CONTENT OF THE DISSERTATION

**In the introduction**, the actuality of the subject of the dissertation, degree of elaboration, purposes and tasks of the research, information about the research methods and objects, the main provisions submitted to the defense, scientific novelty of the study, theoretical and practical significance of the study are described in detail. A list of international and republican level conferences where the results of scientific research were discussed is also presented here.

**In chapter I**, the technological bases of the synthesis, growing of monocrystals and obtaining thin films of the compounds  $\text{CuIn}_5\text{S}_8$  and  $\text{Cu}_3\text{In}_5\text{S}_9$ , which are research objects, are reflected, the characteristics, features and technical parameters of the devices assembled and used based on the methods applied in the work are shown. The synthesis of chemical compounds was carried out by filling the components weighed in stoichiometric ratios into a quartz ampoule and melting under vacuum conditions. In growing monocrystals, it was determined that the zone melting method for the  $\text{CuIn}_5\text{S}_8$  compound, and the slow cooling method in a constant temperature gradient furnace for the  $\text{Cu}_3\text{In}_5\text{S}_9$  compound gave better results. The geometric figures characteristic of the corresponding crystal structures on the plane surface of the crystallized ingots are depicted in figure 1.

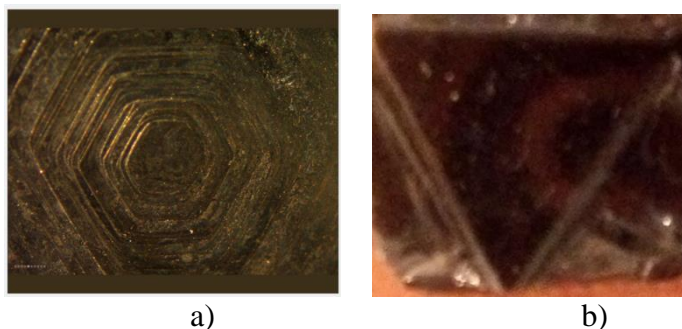


**Figure 1. Figures formed on the surface of  $\text{Cu}_3\text{In}_5\text{S}_9$  (a) and  $\text{CuIn}_5\text{S}_8$  (b) crystals.**

The production of chemical compounds containing a component such as elemental sulfur, which evaporates easily and has a high vapor pressure, by the thermal evaporation method is associated with a number of difficulties. The substance of most binary sulfur compounds decomposes when heated to its melting temperature. Therefore, obtaining a vapor flow corresponding to the stoichiometric composition of the solid phase by thermal evaporation and providing vapor condensation requires the application of a number of technological methods and modes. Thus, traditional technological operations cannot be used for the evaporation of substances that contain an easily volatile component such as sulfur element or chemically active ion that can react at high temperatures with the material of the evaporating furnace and container.

Taking into account the problems and characteristics of vaporization of matter in a vacuum by the thermal method, a number of technological innovations have been applied by us to obtain thin film of  $\text{CuIn}_5\text{S}_8$  and  $\text{Cu}_3\text{In}_5\text{S}_9$  compounds. The synthesized substance was poured into a vacuum-annealed glass cylindrical graphite in the form of  $\sim 100 \mu\text{m}$  powder and deposited on various substrates, including liquid surfaces, by rapid evaporation. Microstructural and spectroscopic analyzes were performed on the obtained thin films.

**Chapter II** is dedicated to the description of the methodology of the methods used to study the electrical, photoelectric and luminescent properties in crystals and thin films in a wide temperature range, optical excitation level and spectrum. An accurate and reliable method for determining the concentration of charge carriers is the Hall effect method. However, a number of problems arise in measuring the Hall voltage in high resistivity crystals such as  $\text{CuIn}_5\text{S}_8$  and  $\text{Cu}_3\text{In}_5\text{S}_9$ . The most difficult of these is the creation of a parasitic potential difference between the Hall contacts due to inhomogeneity in the crystal. In high-resistance crystals, the value of the parasitic voltage can be several orders of magnitude greater than the Hall voltage, which makes it difficult to accurately determine the Hall voltage. Therefore, it is purposeful to use the Hall current method in high resistance crystals. With this method, the Hall

mobility of charge carriers is determined and the concentration is found taking into account the value of electrical conductivity.

Activation energies of 0.48 eV and 1.32 eV were determined from the study of the temperature dependence of the resistivity of the  $\text{CuIn}_5\text{S}_8$  crystal. The first value, 0.48 eV, certainly corresponds to the deep donor level occupancy depth. The second energy value corresponds to the width of the band gap of the  $\text{CuIn}_5\text{S}_8$  crystal. In the literature, different numbers are given for the width of the band gap of the  $\text{CuIn}_5\text{S}_8$  crystal. For example, values in the range of 1.25-1.35 eV are shown for interband direct optical transitions, and values in the range of 1.45-1.52 eV are shown for indirect optic transitions.

From the comparison of the temperature dependence of the electrical conductivities of  $\text{CuInS}_2$  and  $\text{CuIn}_5\text{S}_8$  crystals, the fact that the activation energies of the donor levels are close at 0.454 eV and 0.48 eV, respectively, gives reason to assume that these conductivity mechanisms are of the same nature. If the energy level of 0.454 eV in the  $\text{CuInS}_2$  crystal shows itself to the conductivity starting from the temperature of 320 K, it is observed that the donor level with the energy of 0.48 eV in the  $\text{CuIn}_5\text{S}_8$  crystal appears from the temperature of 250 K. This can be explained by the fact that the donor levels in  $\text{CuInS}_2$  and  $\text{CuIn}_5\text{S}_8$  crystals are mainly due to anion vacancies (sulfur vacancies), and while the  $\text{CuInS}_2$  compound satisfies the normal valence condition, in the  $\text{CuIn}_5\text{S}_8$  crystal, there are 25% vacancies in the anion sublattice of the crystal structure. As a result of the donor-acceptor interaction due to the occupation of anion vacancies by cations, the donor level in the  $\text{CuIn}_5\text{S}_8$  crystal is located in a deeper position than the similar level in the  $\text{CuInS}_2$  crystal. It is the donor-acceptor mutual compensation in the  $\text{CuIn}_5\text{S}_8$  crystal that can be explained as the reason why the crystal has a higher resistivity than the  $\text{CuInS}_2$  crystal.

In the  $\text{CuIn}_5\text{S}_8$  crystal, the Hall mobility of conduction electrons at room temperature is  $27 \text{ cm}^2/\text{V}\cdot\text{s}$ . A  $\mu(T)$  dependence is observed in the 77 – 200 K interval, and a weak  $\mu \sim T$  proportionality is observed in the 200 – 300 K interval (figure 2). It can be assumed that the scattering of charge carriers in the first interval corresponds to scattering from neutral atoms, and in the second interval from

acoustic phonons. Starting from the temperature of 300 K, the temperature dependence of the mobility obeys the law of  $\mu \sim T^{-1,08}$ .

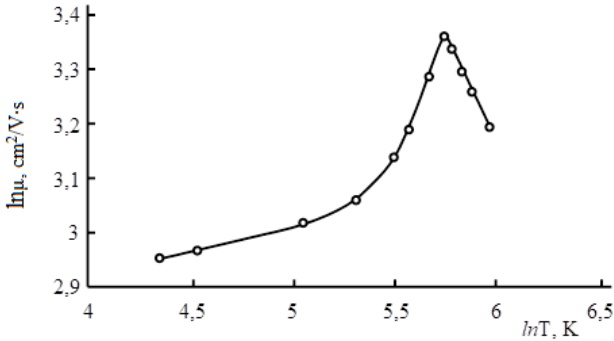


**Figure 2. Temperature dependence of Hall mobility of conduction electrons in CuIn<sub>5</sub>S<sub>8</sub> crystal.**

In the Cu<sub>3</sub>In<sub>5</sub>S<sub>9</sub> crystal, two parts obeying the exponential law in the dependence of  $\lg \sigma \sim 1000/T$  were observed, and the activation energies of charge carriers corresponding to these parts were calculated. Considering that the crystal has n-type conductivity, the levels are assumed to be of donor type. According to the calculations, there are two donor impurity energy levels in the crystal with a depth of 0.28 eV and 0.76 eV. The deviations from the exponential character in the  $\sigma(\tau)$  dependence in the temperature interval of 240 – 270 K and above 360 K are explained by the complex nature of the temperature dependence of the charge carriers in the crystal. The temperature dependence of the Hall mobility of electrons in the Cu<sub>3</sub>In<sub>5</sub>S<sub>9</sub> crystal is depicted in figure 3 on a double logarithmic scale. As it can be seen, the characteristic form of  $\mu(T)$  dependence shows similarity with the corresponding character of electron mobility in CuIn<sub>5</sub>S<sub>8</sub> crystal. However, starting from the temperature of 200 K in the Cu<sub>3</sub>In<sub>5</sub>S<sub>9</sub> crystal,  $\mu(T)$  dependence turns out that the mechanism of scattering of electrons from optical phonons works. Because the Cu<sub>3</sub>In<sub>5</sub>S<sub>9</sub> crystal has a layered structure, a complex technological regime is not required for perfect crystal growth. On the other hand, while the CuIn<sub>5</sub>S<sub>8</sub> crystal has 25% vacancies in the anion sublattice, such vacancies are 11.6% in the Cu<sub>3</sub>In<sub>5</sub>S<sub>9</sub> crystal. Therefore, in

perfectly structured crystals, various scattering mechanisms play a dominant role in specific temperature ranges.

The Hall effect in the  $\text{Cu}_3\text{In}_5\text{S}_9$  crystal was studied by the Hall current method. It is known that the mobility of electrons in semiconductors is a power function of temperature. It is possible to make an opinion about the scattering mechanism of charge carriers by determining  $n$ -above the graph of this dependence on a double logarithmic scale (figure3). As can be seen from the graph, the dependence of  $\lg \mu$   $\lg T$  in the temperature intervals of 150...250 K and 270...370 K is linear.

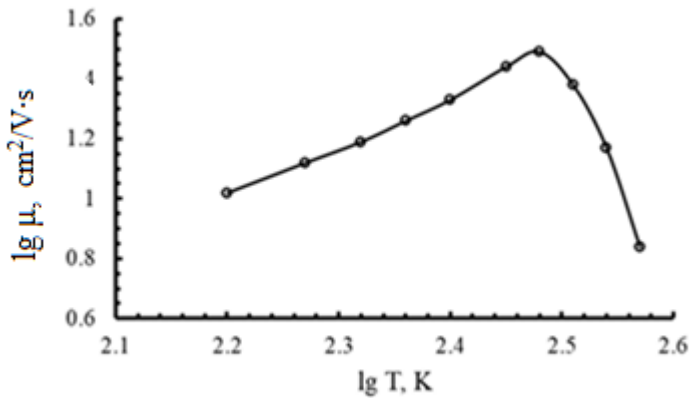


**Figure 3. Temperature dependence of Hall mobility of electrons in  $\text{Cu}_3\text{In}_5\text{S}_9$  crystal.**

In the first interval, the value of  $n=1.5$  is obtained from the slope of the line, which corresponds to scattering of electrons from ionized impurity centers. In the second temperature interval, the mobility decreases sharply with increasing temperature,  $n = -0,5$  is calculated from the slope of the line. Therefore, the scattering mechanism of electrons in the high temperature range corresponds to scattering from optical phonons.

**Chapter III** deals with studies of optical absorption, photoelectric and luminescent properties of  $\text{CuIn}_5\text{S}_8$  and  $\text{Cu}_3\text{In}_5\text{S}_9$  crystal samples and thin films. The spectrum of the photoconductivity of the  $\text{CuIn}_5\text{S}_8$  crystal at a temperature of 300 K is

depicted in figure 4. The long-wavelength edge of the photocurrent spectrum increases sharply in the range starting from 0.8 eV energy to 0.98 eV energy. We consider this to be the current of non-equilibrium charge carriers created by the transition of electrons in the valence band to numerous small donor levels and electrons localized in the acceptor level to the conduction band under the influence of light. From the temperature dependence of electrical conductivity, the activation energy of charge carriers was determined to be 0.48 eV. Therefore, we consider the energy of 0.98 eV as the release energy of electrons localized at the acceptor level. It can be considered that the photocurrent decays linearly in the fundamental absorption band. This may be caused by the property of the surface states of the crystal. The visible curvature in the spectrum at 1.5 eV is probably photoconductivity stimulated by an indirect optical transition in the crystal.

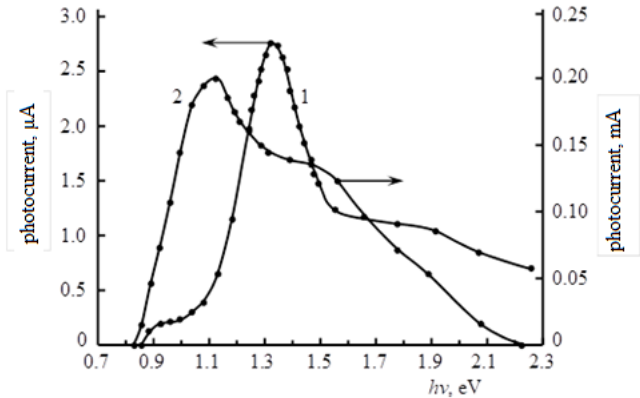


**Figure 4. Spectra of photocurrent at 140(1) and 300(2) K in  $\text{CuIn}_5\text{S}_8$  crystal**

As the crystal cools, the dynamics of the spectrum of photoconductivity changes dramatically. The spectrum of the photoconductivity of the  $\text{CuIn}_5\text{S}_8$  crystal at 140 K, bringing to a per unit quantum, is depicted in the figure 4 (curve 2). Weak impurity photoconductivity is observed in the long-wavelength region of the spectrum. At low temperatures, the transition probability of electrons

from the valence band to the acceptor level is small, so the electrons cannot be localized at the acceptor level and the impurity photoconductivity at the energy of 0.98 eV become weakened. In this case, the specific photoconductivity increases due to the increase in the lifetime of non-equilibrium charge carriers. The amplitude of the maximum increases sharply and a peak corresponding to the specific photoconductivity is observed at an energy of 1.31 eV. A maximum with a large radius of curvature appears around the energy of 2 eV, and at a temperature of 100 K, an impurity photoconductivity at an energy of 0.98 eV and a curvature in the spectrum at an energy of 2 eV is clearly evident, which is explained by the contribution of electrons to the photoconductivity by moving to the subband with a low effective mass.

CuIn<sub>5</sub>S<sub>8</sub> crystal has a defective crystal structure. It is a defective crystal belonging to space group Oh7(Fd3m) with spinel structure and 25% vacancies in its cation sublattice. Against the background of a large amount of anion-cation vacancies, the physical properties of the CuIn<sub>5</sub>S<sub>8</sub> crystal are not strongly influenced by foreign impurity atoms. On the other hand, anion-cation vacancies change the energy spectra of electronic states in the crystal and lead to the creation of electron-hole pairs localized at the donor and acceptor levels. Therefore, in addition to specific absorption in the crystal, additive absorption also enriches its optical and photoelectric properties. In the fundamental absorption region of the CuIn<sub>5</sub>S<sub>8</sub> crystal, the absorption coefficient is 10<sup>5</sup> cm<sup>-1</sup>, and the photosensitivity region covers the main region (1.1-3.2 eV) of the energy spectrum of the Solar at the earth's surface. Therefore, CuIn<sub>5</sub>S<sub>8</sub> is used in photoelectronics in the form of powder and thin film.

In this work, a thin film of CuIn<sub>5</sub>S<sub>8</sub> was obtained by rapid thermal evaporation in vacuum. A mixture of primary components with a total mass of 20 g in a proportion corresponding to the stoichiometric CuIn<sub>5</sub>S<sub>8</sub> composition was synthesized by directly melting in an ampoule. After the synthesis, the substance had a polycrystalline structure. 4-5 g of the substance was ground into a powder with an average size of 100 μm. The powders poured into the graphite furnace heated to 200<sup>0</sup>C in a vacuum by the use of a special

device were rapidly evaporated and deposited on the substrate. Clean glass with  $In_2O_3$  deposited on its surface was used as a substrate plate. The photocurrent spectrum of the layer obtained by this method, calculated per unit quantum, is depicted in figure 5. The photosensitivity region of the  $CuIn_5S_8$  thin film covers the energy range of 0.8÷1.8 eV. The maximum of the spectrum is located at an energy of 1.23 eV. It is determined from the analysis of scientific works that the photoelectric and optical properties of the  $CuIn_5S_8$  crystal strongly depend on the concentration of anion and cation vacancies of the crystal structure. In the spectrum depicted in Figure 5, the long-wavelength edge of the photocurrent does not conform to Moss rule and has a widespread shape. The energy corresponding to the maximum of the spectrum corresponds to the energy between the donor-acceptor levels (1.23 eV).

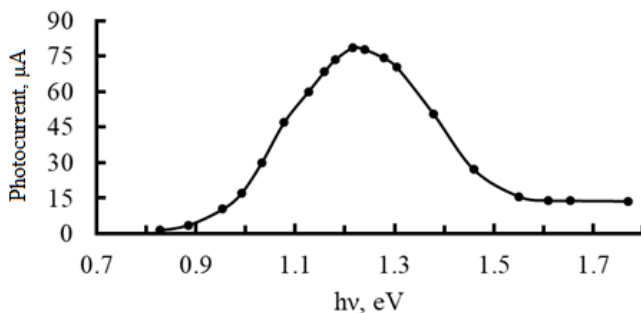
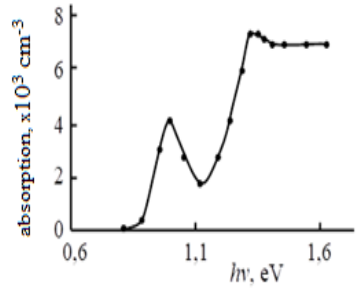


**Figure 5. Spectra of photocurrent calculated per unit quantum of  $CuIn_5S_8$  thin film grown on glass with  $In_2O_3$  deposited on its surface**

Figure 6 shows the spectrum of the absorption coefficient of the  $CuIn_5S_8$  layer grown on the liquid oil surface and obtained as a result of washing the oil liquid and depositing it on the metal grid.



a)



b)

**Figure 6. Absorption coefficient spectrum (b) of  $\text{CuIn}_5\text{S}_8$  film grown on liquid oil surface and obtained as a result of washing the oil liquid and depositing it on a metal grid (a).**

The thickness of the thin film was  $1.2 \mu\text{m}$ . Measuring the absorption coefficient at values of  $10^4 \text{ cm}^{-1}$  and more in such a thin layer does not cause approximate difficulties. Therefore, it was possible to study the spectrum of the absorption coefficient of  $\text{CuIn}_5\text{S}_8$  thin film in the fundamental absorption region. As can be seen from figure 6, a peak is observed in the absorption spectrum at the photon energy of 1.1 eV, and the fundamental absorption band begins from the energy of 1.1 eV. The 0.99 eV energy peak observed in the spectrum is explained by the optical absorption occurring between the levels formed due to the donor and acceptor vacancies in the crystal. As mentioned above, in the  $\text{CuIn}_5\text{S}_8$  crystal structure, there is a 25% vacancy in the cation sublattice, and an anion vacancy is formed in a large amount, so that the donor-acceptor interaction in the crystal plays an important role in the optical, photoelectric and electrical properties of the crystal and forms various properties. Therefore, we explain the peak with an energy of 0.99 eV by the transfer of electrons in compensated acceptor levels to the donor level by absorbing photons of the appropriate energy.

The temperature dependence of the photocurrent caused by photons with energy corresponding to the maximum of the spectrum of the photocurrent of  $\text{CuIn}_5\text{S}_8$  thin film brought to a per unit quantum is depicted in figure 7. In the temperature range of 80...600 K, the photosensitivity of the sample increases regularly, and in the

range of 80...480 K, the dependence is almost linear. Such a feature of photocurrent is important for the development of photodetectors that can operate in the optical and temperature ranges shown in the  $\text{CuIn}_5\text{S}_8$  thin film. The change of the photoconductivity of the  $\text{CuIn}_5\text{S}_8$  thin film by two orders of magnitude compared to the dark conductivity indicates that the film can be successfully applied in the preparation of high-efficiency photocatalysts.

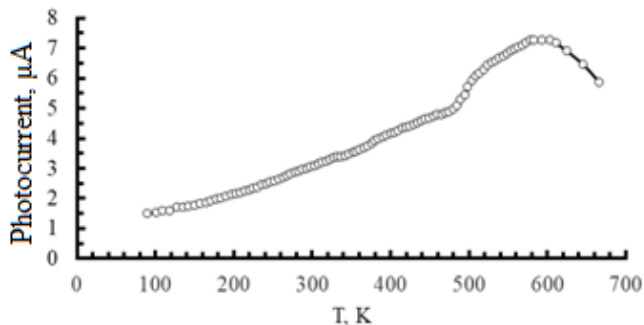


**Figure 7. Temperature dependence of the photocurrent caused by photons with energy corresponding to the maximum of the spectrum of the photocurrent of the  $\text{CuIn}_5\text{S}_8$  thin film.**

Our research showed that the  $\text{CuIn}_5\text{S}_8$  crystal and thin film is a promising material for the production of wideband and high-efficiency photoconverters that can operate in the energy range of photons of natural radiation  $h\nu = 0.8...2.7$  eV.

Spectra of photoconductivity (PC) calculated per unit quantum of  $\text{Cu}_3\text{In}_5\text{S}_9$  crystal at different temperatures are depicted in figure 8. As you can see, the spectrum covers the energy range of electromagnetic radiation of 0.9...2.5 eV. The main part of the spectrum of solar radiation on the earth's surface is also located in this range. Therefore, the  $\text{Cu}_3\text{In}_5\text{S}_9$  crystal can be used in the preparation of an effective converter of solar radiation.

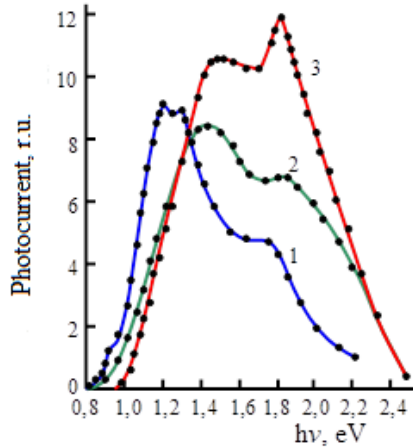


**Figure 8. Spectra of photoconductivity of  $\text{Cu}_3\text{In}_5\text{S}_9$  crystal at different temperatures: 1- 114 K; 2- 210 K; 3- 295 K.**

The dynamics of the change of the spectrum of the photocurrent depending on the temperature is complex. At low temperature (curve 1), the long-wavelength edge of the spectrum is sharp and the structure is observed at an energy of 0.96 eV. The maximum of the spectrum was formed by two peaks with energies of 1.22 and 1.28 eV. These peaks cannot be attributed to the photoconductivity caused by interband transitions, because the temperature coefficient of the band gap of the crystal ( $E_g=1.55\text{eV}$ ) has a negative sign, so the edge in the PC spectrum shifts to a low energy side as the temperature decreases.

At temperatures of 210 and 295 K, new peaks appear in the high energy region of the spectra, and their intensities increase sharply as the temperature increases.

Based on the temperature dependence of the electrical conductivity of the crystal, donor levels with a depth of 0.28 and 0.76 eV were detected. Since the shallow donor levels are empty at low temperatures, the transfer of electrons from the valence band to these levels creates impurity photoconductivity. Therefore, PC observed in the energy range of 0.9 and 1.5 eV can be attributed to the donor-acceptor levels formed by anion-cation vacancies.

The photoconductivity in the  $\text{Cu}_3\text{In}_5\text{S}_9$  crystal was studied under the conditions of constant illumination of the sample in the stationary mode and under the influence of the pulse of the second harmonic ( $\lambda=532\text{nm}$ ) of  $\text{Nd}^{+3}:\text{YAG}$  laser radiation with a duration of 12 ns. The kinetics of the photocurrent generated under the influence of the laser beam pulse is illustrated in figure 9.



**Figure 9. Kinetics of photocurrent in  $\text{Cu}_3\text{In}_5\text{S}_9$  crystal.**

Despite the interruption of the laser pulse for 12 ns, it is observed that the generation of photocurrent continues in the crystal. The  $\text{Cu}_3\text{In}_5\text{S}_9$  crystal has a defective structure, that is, 11.6% vacancies exist in the anionic sublattice. Considering that the crystal has n-type conductivity, it is possible that the concentration of the donor-acceptor pair is high. In this case, the neutralization of the ionized acceptors under the influence of the laser beam and the acceptance of the valence band electrons by the neutral acceptors after the radiation is stopped leads to an increase in the concentration of non-equilibrium holes, thereby increasing the photocurrent. Photocurrent relaxation goes through fast and slow recombination centers. The lifetime of the fast recombination centers is 20 ns, which makes it possible to use the  $\text{Cu}_3\text{In}_5\text{S}_9$  crystal as a high-frequency photoelectric converter. A decaying harmonic dependence is also

observed in the photocurrent relaxation curve, which can be explained by the formation of drift capacitance in the sample under the influence of the laser beam. As observed in the InSe ultrathin film, the drift capacitance arises in the case of a sharp difference in the mobility of non-equilibrium electrons and holes.

Taking into account that the value of the band gap of the  $\text{Cu}_3\text{In}_5\text{S}_9$  crystal is 1.55 eV according to the absorption spectrum, the crystal was excited by the 2nd harmonic of the laser radiation. The photoluminescence spectrum of the  $\text{Cu}_3\text{In}_5\text{S}_9$  crystal excited by a  $\lambda=532$  nm wavelength pulse of laser radiation with an intensity of  $4 \cdot 10^{16}$  quant/cm<sup>2</sup>·s is depicted in figure 10. Numerous structures were observed in the spectrum. The wideband radiation observed around 1000 nm can be associated with the optical transition between the acceptor-donor levels with an energy of 1.05 eV observed in the spectrum of the absorption coefficient of the  $\text{Cu}_3\text{In}_5\text{S}_9$  crystal. The observation of this band at low intensities of excitation laser radiation and the disappearance of the radiation band with increasing intensity can be explained by the complete discharging of the donor level at high intensities of laser radiation.

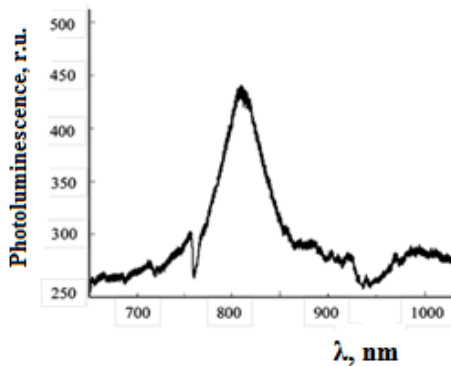


**Figure 10. Photoluminescence spectrum of the  $\text{Cu}_3\text{In}_5\text{S}_9$  crystal excited by a  $\lambda=532$  nm wavelength pulse of laser radiation with an intensity of  $4 \cdot 10^{16}$  quant/cm<sup>2</sup>·s**

Figure 11 shows the photoluminescence spectrum on the naturally formed mirror surface during the  $\text{CuIn}_5\text{S}_8$  crystal growth

process. Curves 1 and 2 are the luminescence spectra by exciting the crystal with a pulse of laser radiation with a photon flux of density  $5 \cdot 10^{22} \text{ cm}^{-2}\text{s}^{-1}$  and  $3 \cdot 10^{24} \text{ cm}^{-2}\text{s}^{-1}$ , respectively. Three characteristic radiation bands are distinguished in the spectra at energies of 1.52 eV (815 nm), 1.48 eV (837 nm) and 1.465 eV (846 nm). From the comparison of the luminescence spectra in the excitation with two different intensities, it can be seen that the 1.52 eV energy band shifts towards the short-wave region with increasing intensity. Some articles in scientific journals show that the  $\text{CuIn}_5\text{S}_8$  crystal has a direct bandgap at an energy of 1.51 eV.

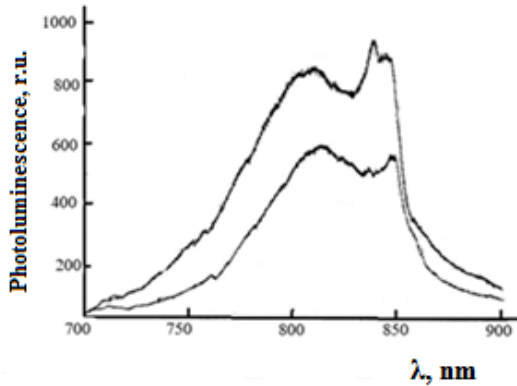


**Figure 11. Photoluminescence spectrum on a naturally formed mirror surface in the process of growing  $\text{CuIn}_5\text{S}_8$  crystal.**

Due to the Burstein-Moss effect in semiconductors at a high level of optical excitation, the luminescence spectrum shifts to the short-wave region with the increase in the excitation intensity. The lower the state density of electrons in the subband of the edges of valence and conduction bands, where the direct optical transition occurs, the weaker the dependence of the spectrum shift on the intensity. According to the expression of the density of states in the bands, it is expressed as follows for the valence electron:

$$N_p = 2 \left( \frac{2\pi\omega_p kT}{h^2} \right)^{3/2} \quad (1)$$

As a result, the maximum intensity of the spectra at 1.52 eV energy is slightly shifted by 2 order changes. Therefore, in the considered subbands, the effective mass of the charge carriers is large, and the drift mobility is small. This consideration can be attributed primarily to the corresponding subband at the maximum of the valence band. Because it was shown in the second chapter that the mobility of electrons in the CuIn<sub>5</sub>S<sub>8</sub> crystal is quite large, that is, the electrons that play the main role in conductivity locate in the subband of the conduction band, which forms the 1.31 eV width of the indirect band gap. Thus, we came to the conclusion that the drift mobilities of conducting electrons and holes in the CuIn<sub>5</sub>S<sub>8</sub> crystal differ sharply from each other. This result we obtained is the evidence confirming the occurrence of drift capacitance in the crystal under conditions of high optical excitation and the explanation of the features in the photocurrent relaxation curves.

In figure 11, the radiation bands at 1.48 and 1.465 eV energies in the luminescence spectra do not change their position according to the energy with the change of laser radiation intensity, but the intensities of the bands change sharply. The peak at 1.48 (837 nm) eV energy grows more sharply with increasing excitation level. We assume that the radiation bands at energies of 1.48 and 1.465 eV are formed due to direct optical transitions of non-equilibrium electrons from the conduction band to the acceptor levels.

The increase in the photon flux emitted by the high optical excitation of the crystal is a product of the short-term recombination process, in which case a nanosecond relaxation of the photocurrent is observed in the crystal. When the radiative recombination mechanism works, the emitted photon flux is expressed as:

$$\rho_V(t, \omega) = \frac{\omega_V^2}{2\pi\hbar v^2} \quad (2)$$

Here,  $\omega_V = v_V \cdot q_V$ ,  $v_V$  is the phase speed,  $q_V$  is the wave vector,  $v$  is the speed of light propagation in the crystal. From the formula (2), it is obtained that the smaller the speed of light propagation in the crystal, the greater the density of radiated photons. This observation agrees with the result obtained for the CuIn<sub>5</sub>S<sub>8</sub> crystal in this study. It is shown that the refractive index in the CuIn<sub>5</sub>S<sub>8</sub> crystal takes large values.

Figure 12 shows the luminescence spectrum of the CuIn<sub>5</sub>S<sub>8</sub> thin film grown by the thermal evaporation method in vacuum on the liquid oil surface. Unlike the luminescence spectrum of a crystal ingot, the luminescence spectrum of a thin film covers a narrow range of electromagnetic waves (855 ... 885 nm). First of all, the shape of the spectrum of the radiation band attracts attention: at the high energy edge, the spectrum falls off sharply, and the linear extrapolation of this part of the fall corresponds to an energy of 1.449 eV at the intersection with the energy axis.

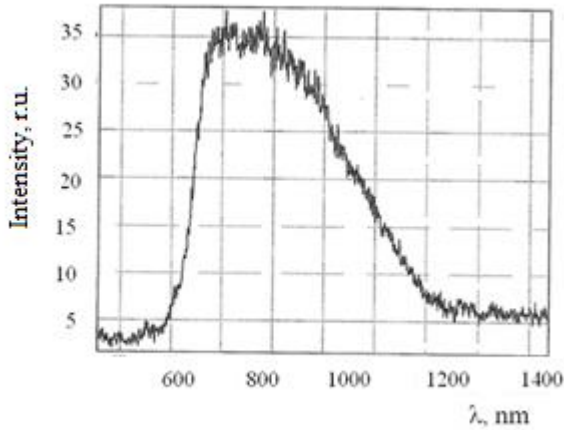


**Figure 12. Luminescence spectrum of CuIn<sub>5</sub>S<sub>8</sub> thin film grown by thermal evaporation in vacuum on liquid oil surface.**

The decrease in radiation intensity in the wavelength range of 860 ... 880 nm is exponential. In a perfectly pure crystalline structure, the efficiency of photoluminescence is proportional to its intensity and is expressed by the following equation:

$$\eta = \frac{1}{a} \int \psi(\nu) [1 - e^{-\alpha(\nu)\alpha}] d\nu \quad (3)$$

Here,  $a$  is the two photon absorption probability,  $\psi(\nu)$  is the fluorescence spectrum,  $\alpha(\nu)$  is the absorption spectrum. The correspondence of the fluorescence spectrum observed in the CuIn<sub>5</sub>S<sub>8</sub> thin film to the equation (3) is proof that the structure of the thin film

is perfectly pure. The interpretation of such a spectrum is carried out according to the configuration diagram created on the basis of the French-Condon principle.

**Chapter IV** describes the preparation of photocatalysts based on  $\text{CuIn}_5\text{S}_8$  and  $\text{Cu}_3\text{In}_5\text{S}_9$  thin films with a nanoparticle surface and their use in hydrogen production by water splitting. Due to their unique properties and characteristics, Ag nanoparticles have received much attention in the last few decades. Due to their optical properties, silver nanoparticles exhibit localized surface plasmon resonance, making them suitable for biomedical visualization in near-field optical probes and contrast agents. The size of nanoparticles plays an important role in various application fields. Therefore, obtaining controlled-sized Ag nanoparticles and keeping them in a stabilizing environment for a long time is one of the important issues of nanotechnology. In a number of photocatalytic reactions and biophysical studies, complex experiments in electrolytic media and the study of various functional combinations of antibody/antigen traditional groups require more stable nanoparticles. Studies have shown that peptides exhibit an unusual stabilizing property for silver nanoparticles and at the same time a wide universal method of specific functionalization of nanoparticles.

The polyol synthesis method of Ag nanoparticles has the following advantages over other chemical synthesis methods:

- polyol solids have good solubility in water;
- implementation of the process at temperatures that are not too high ( $\sim 300^\circ\text{C}$ );
- use of metals with a reduction property;
- the ability to form coatings with different functions on nanoparticles.

The polyol process used to synthesize Ag nanoparticles was conducted in a mini reactor. A magnetic mixer was used for mixing the solution inside the reactor. A glass-covered ferromagnetic rod was used as a stirring wing. As a polyol substance, diatomic alcohol, ethylene glycol (EG) ( $\text{HO} - \text{CH}_2 - \text{CH}_2 - \text{OH}$ ) was taken.  $\text{CuCl}_2 \cdot 2\text{H}_2\text{O}$  solution was added to the solution in order to prevent oxidation in the process of Ag cell formation and growth. The

reactant,  $\text{AgNO}_3$  salt, has of high purity. Polyvinylpyrrolidone solution dissolved in ethanol was poured into the reactor to stabilize the formed nanoparticles of the required size. First, 5 ml of ethylene glycol (EG) with a boiling point of  $175^\circ\text{C}$  was poured into the reactor and heated to a temperature of  $155^\circ\text{C}$  and mixed for 1 hour at a speed of 260 revolutions/minute of a magnetic stirrer. Images of the distribution of nanoparticles on the surface of  $\text{CuIn}_5\text{S}_8$  and  $\text{Cu}_3\text{In}_5\text{S}_9$  thin films were observed in figure 13. The image was taken on an optical microscope manufactured by "Carl Zeiss" and equipped with a high-resolution camera. Bright spots are attributed to Ag nanoparticles. A diffraction image similar to Newton's rings is observed near the surface of the thin film at X2000 magnification of the image taken in the mode of reflection rays from the surface. The formation of light rings of different colors can be assumed to be due to the interference pattern created by the rays reflected from the surface of the nanoparticle and falling on the surface of the thin layer and reflected directly to the surface of the thin layer. While in Newton's rings the central part is bright, the image we observed appeared to consist of a dark circle at high magnification. It can be said that the Ag nanoparticles grown by us are in an ideal spherical shape.

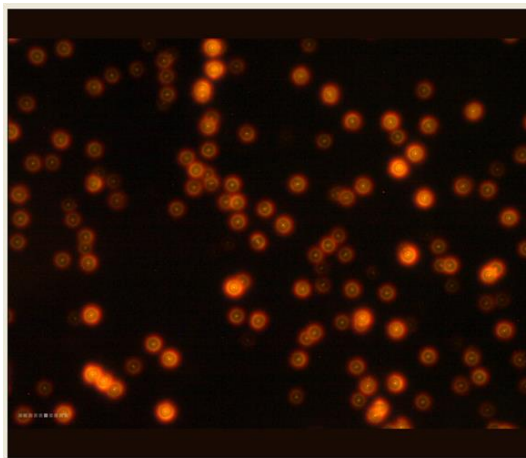


**Figure 13. Diffraction image similar to Newton's rings near the surface of nanoparticles on the surface of  $\text{CuIn}_5\text{S}_8$  thin films (X800).**

A schematic representation of the electrolytic bath and electrodes used to perform the electrolytic water splitting is depicted in figure 14. The electrolytic bath consists of a transparent, rectangular plastic container with a closed mouth. Electrodes are attached to the lid of the container and electrical contacts are connected. A small opening is made on the platinum electrode to allow hydrogen gas to exit. An electrolytic bath is placed on an analytical balance. The electrodes are connected to a constant current source equipped with a voltmeter and an ammeter. Figure 14 shows a visual representation of the electrolysis bath.

In order to create a nanoparticle surface on the electrode with a positive potential, a drop of the colloidal solution of Ag nanoparticles in ethanol was poured onto the surface of the glass / p – Ge / CuIn<sub>5</sub>S<sub>8</sub> structured electrode prepared by the method described above, and it was shaken in a vibrator to evenly distribute it on the surface. Then the electrode was kept in a vacuum at a temperature of 200°C for 2 hours. At this technological stage, adhesion of Ag-nanoparticles on the surface of CuIn<sub>5</sub>S<sub>8</sub> thin layer was ensured.

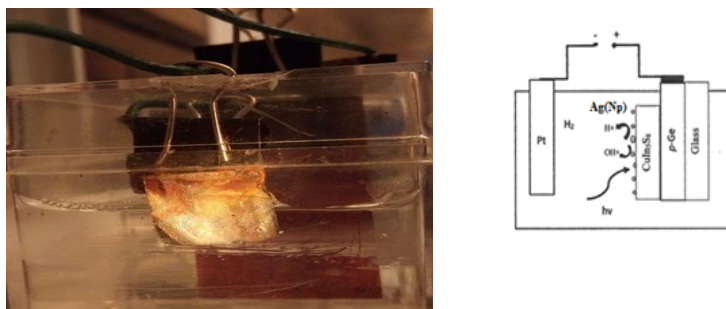


**Figure 14. Schematic representation of the electrolytic bath and electrodes used in the electrolytic water splitting.**

10 ... 12 seconds after the start of the reaction, the image of H<sub>2</sub> gas bubbles formed on platinum is given. The energy consumption of the electric current passing through the electrodes for 6 hours was 15 W•h. When the voltage applied to the electrodes was 50, the electric

current was 50 mA. Therefore, the electrical energy used in 6 hours is  $W_E = 15 \text{ W}\cdot\text{h}$ . Taking into account that the heat of combustion of hydrogen is  $120 \cdot 10^6 \text{ J/kg}$ , we get that the released 18 mg of hydrogen will give 1820 calories of heat. Therefore, the efficiency of the photocatalytic reaction is 5 without considering the light energy.

$$\eta = \frac{W_H}{W_E} \cdot 100 = 3,6\%$$

without considering the light energy. Such efficiency was also obtained in the reaction with Zn/CuIn<sub>5</sub>S<sub>8</sub>/TiO<sub>2</sub> structure photocatalyst electrode.

A colloidal solution of TiO<sub>2</sub> nanoparticles in water was prepared and a small amount of the product was homogeneously distributed on the surface of the thin layer of CuIn<sub>5</sub>S<sub>8</sub> and subjected to thermal annealing at 200°C under vacuum conditions for 3 hours. The durability of the photocatalyst prepared by this method and using a thin layer of Zn as a buffer layer in the electrolysis process was 18 hours. However, the photocatalyst with glass / p – Ge/CuIn<sub>5</sub>S<sub>8</sub> /Ag (Np) structure was 3.2% efficient in H<sub>2</sub> production by water splitting, and the reaction endurance time was more than 72 hours.

## MAIN RESULTS

1. In the n -  $\text{CuIn}_5\text{S}_8$  crystal with defect structure, vacancies in the cation sublattice and the depth of the impurity level were determined to be 0.48 eV, and the electrons directly transitioning from the valence band to the minimum of the conduction band by 1.35 eV play a key role in the electrical conductivity in the crystal in the temperature range of 77 – 380 K . Conduction electrons in the  $\text{CuIn}_5\text{S}_8$  crystal are scattered from neutral impurity atoms in the temperature range of 77 – 200 K, from acoustic phonons in the range of 200 – 300 K, and from acoustic and optical phonons in the range of 300 – 380 K, which correspond to the mixed scattering mechanism.

2. The current conduction mechanism of  $\text{Cu}_3\text{In}_5\text{S}_9$  monocrystal in the temperature range of 100 – 370 K is formed by the activation of electrons from the donor levels with a depth of 0.28 and 0.76 eV, electron scattering is conform by neutral impurity atoms in the range of 150 – 250 K, and in the range of 270 – 370 K, is conform to scattering mechanism by optical phonons.

3. The open circuit voltage  $V_{OC} = 0.385$  V and the short circuit current  $I_{SC} = 6.75$  mA when the p-Si/n- $\text{CuIn}_5\text{S}_8$  tandem photocell is illuminated with solar radiation by the  $\text{CuIn}_5\text{S}_8$  thin film under AMO conditions, the value calculated for the fill factor coefficient (f.f.) of VAC: f.f.= 56%, the photocell has great practical interest in order to develop a high-efficiency converter for the conversion of solar radiation into electrical energy.

4. In the  $\text{Cu}_3\text{In}_5\text{S}_9$  crystal, under the influence of the pulse of the second harmonic ( $\lambda=535$  nm) of  $\text{Nd}^{+3}$ :YAG laser radiation, the duration of which is 12 ns, the relaxation of the photocurrent goes through fast and slow recombination centers. The lifetime of the fast recombination centers is 20 ns, so the  $\text{Cu}_3\text{In}_5\text{S}_9$  crystal can be used as a high-frequency photoelectric converter.

5. The maximum of the intense radiation band of the  $\text{Cu}_3\text{In}_5\text{S}_9$  crystal is located at an energy of 1.53 eV, which is considered equal to the width of the band gap of the crystal at room temperature. The formation of the extreme minimum at the wavelength of 758 nm

(1.636 eV) in the spectrum can be explained by a certain amount of localization of excited electrons at 1.636 eV. The subband located in the conduction band at such a height from the ceiling of the valence band allows the formation of triplet excitons in the crystal.

**6.** By exciting the  $\text{CuIn}_5\text{S}_8$  crystal with a photon flux with a density of  $5 \cdot 10^{22} \text{ cm}^{-2}\text{s}^{-1}$  and  $3 \cdot 10^{24} \text{ cm}^{-2}\text{s}^{-1}$  in the luminescence spectra of 1.52 eV (815 nm), 1.48 (837 nm) and 1.465 (846 nm) energies, three characteristic radiation bands were observed. The radiation bands at the energies of 1.48 and 1.465 eV are formed due to the direct optical transition of non-equilibrium electrons from the conduction band to the acceptor levels. The formation of drift capacitance in the crystal under conditions of high optical excitation due to sharp differences in the drift mobility of conducting electrons and holes in the crystal is the reason for the formation of features in the relaxation curves of the photocurrent.

**7.** It was observed that Ag-nanoparticles on the surface of  $\text{CuIn}_5\text{S}_8$  and  $\text{Cu}_3\text{In}_5\text{S}_9$  thin films produce a diffraction image similar to Newton's rings near the surface of the thin film. It was assumed that the formation of light rings of different colors occurs due to the interference pattern created by the rays that fall on the surface of the thin layer and reflect from the surface of the nanoparticle and the rays that reflect directly to the surface of the thin layer. It can be said that the Ag nanoparticles grown by us are spherical in shape.

**8.** In the reaction with  $\text{Zn/CuIn}_5\text{S}_8/\text{TiO}_2$  structured photocatalyst electrode, the efficiency of the reaction in  $\text{H}_2$  production by water splitting was 3.6%, the efficiency in  $\text{H}_2$  production by water splitting of the p-Ge/ $\text{CuIn}_5\text{S}_8/\text{Ag}(\text{Np})$  structured photocatalyst was 3.2%, and the reaction endurance time was more than 72 hours. The efficiency of the reaction in the production of  $\text{H}_2$  by water splitting with a positive potential electrode with a  $\text{Zn/Cu}_3\text{In}_5\text{S}_9/\text{Ag}(\text{Np})$  photocatalyst was determined to be 2.9%. The low surface roughness of  $\text{Cu}_3\text{In}_5\text{S}_9$  thin films leads to low efficiency of electrolysis.

## LIST OF SCIENTIFIC WORK PUBLISHED ON DISSERTATION SUBJECT

1. A.G.Guseinov, V.M.Salmanov, R.M.Mamedov, A.Z.Magomedov, A.İ.Bayramova, Specific Features of Photoluminescence and Nanosecond Relaxation of Photocurrent in  $\text{CuIn}_5\text{S}_8$  Crystals upon Strong Optical Excitation, Optics and Spectroscopy, Pleiades Publishing, Ltd. 2020, s.1983–1987

2. Bayramova A.İ. Photovoltaic energy converters based on n- $\text{CuIn}_5\text{S}_8$  -p-Si heterostructure, Bakı Universitetinin Xəbərləri, Fizika-Riyaziyyat elmləri seriyası, 2021, s.118-122

3. A. G. Guseinov, A.İ. Bayramova, Preparation and properties of photosensitive  $\text{Cu}_3\text{In}_5\text{S}_9$  thin films, AJP FIZIKA, 2023, s.11-13

4. A. G. Guseinov, A.İ. Bayramova, Thermal quenching of photocurrent in  $\text{CuIn}_5\text{S}_8$ , Journal of Baku Engineering University PHYSICS, 2023, s.45-48

5. A.G.Guseinov, R.M.Mamedov, A.İ.Bayramova, M.M. Javadova, Features of the Dynamics of the Photoluminescence Spectrum of the  $\text{Cu}_3\text{In}_5\text{S}_9$  Crystal with a Change in the Intensity of Laser Excitation, Optics and Spectroscopy, 2022, s.1201-1204

6. A.İ.Bayramova,  $\text{CuIn}_5\text{S}_8$  nazik təbəqəsində fotocərəyanın xüsusiyyətləri, Ekologiya və su təsərrüfatı jurnalı, AzMİU, 2020, s.59-61

7. A.İ.Bayramova, Thermostimulated conductivity and impurity absorption in  $\text{CuIn}_5\text{S}_8$ , Journal of Baku Engineering University Chemistry and Biology, 2021, s.54-58

8. T.M. Pənahov, Ə.H.Hüseynov, A.İ.Bayramova,  $\text{CuIn}_5\text{S}_8$  kristalında fotoluminesensiya və fotokeçiricilik, Azərbaycan Xalq Cümhuriyyətinin yaranmasının 100 illiyinə həsr olunmuş professor-müəllim heyətinin, doktorantların və gənc tədqiqatçıların Beynəlxalq elmi konfransının materialları, 26-27 aprel, 2018, AzMİU, s.477-480

9. A.İ.Bayramova,  $\text{CuIn}_5\text{S}_8$  kristalında fotoelektrik hadisəsinin xüsusiyyətləri, Azərbaycan Respublikası Təhsil Nazirliyi Doktorantların və Gənc tədqiqatçıların XXII Respublika Elmi konfransı, 2018, s.44-46

10. Ə.H.Hüseynov, V.M.Salmanov, M.B. Cəfərov, R.M. Mamedov, A.İ.Bayramova, Особенности фотоэлектрических свойств  $Cu_3In_5S_9$ , Azərbaycan Respublikası Təhsil Nazirliyi Gəncə Dövlət Universiteti Beynəlxalq Elmi Konfransı, Müasir təbiət və iqtisad elmlərinin aktual problemləri, IV hissə, 03-04 may, 2019, s.253-257

11. A.Г.Гусейнов, В.М. Салманов, Р.М. Мамедов, М.В.Сəfərov, А.А.Салманова, А.İ.Ваурамова, Фотопроводимости и люминесценция кристаллов  $Cu_3Ca_5Se_9$  под действием лазерного излучения, Müasir təbiət elmlərinin aktual problemləri beynəlxalq elmi konfrans 01-02 may III hissə Gəncə, 2020, s.28-34

12. А.Г.Гусейнов, С.С. Рагимов, В.М.Салманов, И.И.Курбанов, А.İ.Ваурамова, Особенности фотопроводимости и фотолюминесценции тонких пленок слоистого кристалла  $Cu_3In_5S_9$ , Министерство науки и высшего образования РФ нанотехнологическое общество России Кабардино–Балкарский Государственный Университет, XII международная научно–техническая конференция микро– и нанотехнологии в электроник, 31 мая–5 июня нальчик, Россия, 2021, s.27-30

13. А.İ.Ваурамова, О.А. Алиев, Фотоэлектрические явления в кристалле  $CuIn_5S_8$ , Azərbaycan Respublikasının Təhsil Nazirliyi, Azərbaycan Memarlıq və İnşaat Universiteti AR Memarlıq,İnşaat elminə və Tədrisin İnkişafına Yardım Xeyriyyə Fondu,Beynəlxalq Elmi-praktik konfrans “Memarlıq və İnşaatda Enerji qoruyucu İnnovasiyalar ESİAC”, 20-21 oktyabr, 2021, s.248-251

14. Т.М.Панахов, А.Г.Гусейнов, А.İ.Ваурамова, Фотоэлектрические преобразователи энергии на основе гетероструктуры  $p-Si$ , Азербайджанский Архитектурно-Строительный Университет “Su təsərrüfatı və mühəndis kommunikasiya sistemlərində innovativ texnologiyalar” Beynəlxalq Elmi-Praktik Konfrans. 08-09 iyun, 2023, s.225-229

The defense will be held **on 12 at June at 15:30** at the meeting of the Dissertation council ED 2.19 of Supreme Attestation Commission the President of the Republic of Azerbaijan operating at Baku State University.

Address: AZ1148, Baku city, Z.Khalilov Street, 23, Baku State University, Main building,

Dissertation is accessible at the Scientific Library of Baku State University.

Electronic versions of the dissertation and its abstract are posted on the official website of Baku State University.

The abstract was sent to the necessary addresses in 8 may 2024.

Seal signed :06.05.2024

Paper format: 210x297 1.4

Volume:43673

Number of hard copies: 20

Printed at “Pixel Print” MMC printing house

Mobile: (050) 612 13 14

(055) 770 26 10